

Disentangling Uncertainty for Safe Social Navigation using Deep Reinforcement Learning

Daniel Flögel^{*1}, Marcos Gómez Villafañe^{*1,2}, Joshua Ransiek¹, and Sören Hohmann³

Abstract—Autonomous mobile robots are increasingly employed in pedestrian-rich environments where safe navigation and appropriate human interaction are crucial. While Deep Reinforcement Learning (DRL) enables socially integrated robot behavior, challenges persist in novel or perturbed scenarios to indicate *when and why* the policy is uncertain. Unknown uncertainty in decision-making can lead to collisions or human discomfort and is one reason why safe and risk-aware navigation is still an open problem. This work introduces a novel approach that integrates *aleatoric*, *epistemic*, and *predictive uncertainty* estimation into a DRL-based navigation framework for uncertainty estimates in decision-making. We, therefore, incorporate Observation-Dependent Variance (ODV) and dropout into the Proximal Policy Optimization (PPO) algorithm. For different types of perturbations, we compare the ability of Deep Ensembles and Monte-Carlo Dropout (MC-Dropout) to estimate the uncertainties of the policy. In uncertain decision-making situations, we propose to change the robot’s social behavior to conservative collision avoidance. The results show that the ODV-PPO algorithm converges faster with better generalization and disentangles the aleatoric and epistemic uncertainties. In addition, the MC-Dropout approach is more sensitive to perturbations and capable to correlate the uncertainty type to the perturbation type better. With the proposed safe action selection scheme, the robot can navigate in perturbed environments with fewer collisions.

I. INTRODUCTION

Autonomous mobile robots are increasingly being deployed in a variety of public pedestrian-rich environments, e.g. pedestrian zones for transport or cleaning [1]–[5], while DRL-based approaches are increasingly used [6]–[9]. These robots not only have socially aware behavior but also become socially integrated to reduce the negative impact on humans [8]. However, there are two fundamental challenges. The first arises through the variety and a priori unknown scenarios caused by the stochastic behavior of humans [10, 11]. The second through the general problem of machine learning-based systems to predict correct actions in unseen scenarios [12, 13]. Since the robot has to choose an action in each step, one risk is a high level of uncertainty in the decision-making process at action selection [14]. As a consequence, the safe and risk-aware social navigation to avoid collisions and human discomfort is still an open problem [7, 15].

The uncertainty in the robot’s decision-making is affected by scenarios the robot has never experienced in training,

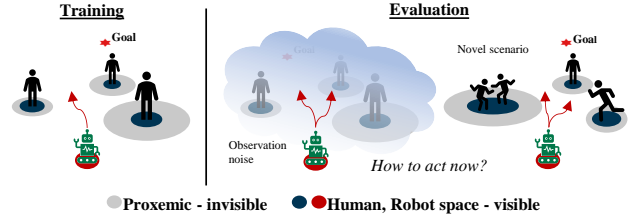


Fig. 1: We propose to integrate aleatoric and epistemic uncertainty estimation of action selection into DRL-based navigation policies to detect scenarios where the robot is uncertain, e.g. due to observation noise or novel scenarios. Depending on the confidence about action selection, the robot either interacts with humans or focuses on safe collision avoidance.

Out-Of-Distribution (OOD) scenarios, and due to the inherent uncertainty of the environment like sensor noise or occlusion [16]. Thus, the DRL policy will face *epistemic uncertainty* (model uncertainty), which correlates with OOD, and *aleatoric uncertainty*, which stems from stochastic environments, e.g. sensor noise or perturbations on selected actions [17]. For a DRL policy, it is essential to estimate both types as it is expected that the robot flags anomalous environmental states when it does not know which action to choose to account for potential risks [17, 18]. Thus, disentangling aleatoric and epistemic uncertainty is crucial for a DRL policy towards safe and risk-aware behavior [18]. However, there is less literature for uncertainty aware DRL, compared to supervised learning [19], and only a few works address the resulting risks in navigation [20].

Most DRL-based navigation approaches, e.g. [8, 21]–[25], do not consider OOD scenarios or noise which is a significant risk since the OOD performance of recent approaches is bad as evaluated in [7]. For known input perturbations, a certified adversarial robustness analysis framework for DRL is proposed in [14]. However, the perturbation must be known a priori, and it only applies to DRL approaches with discrete actions. Other recent works make use of the uncertainty in the human trajectory prediction [2, 9] or propose to detect novel scenarios [13], but neglect the uncertainty in decision-making which is the crucial part [14]. In addition, [13] intentionally replaced PPO [26] with Soft Actor-Critic (SAC) [27] because standard implementations, e.g. [28], of PPO do not have state dependant variance of policy distribution and it is additionally challenging for PPO to train uncertainty-aware behavior while having good exploration-exploitation trade-off. However, many social navigation approaches rely on the PPO algorithm due to the stable training and good performance [5, 8, 9, 16, 29]–[41].

We see the clear limitation that uncertainty in decision-making is neither considered nor the source determined.

^{*} Authors contributed equally: Daniel Flögel, Marcos Gómez Villafañe
¹ are with FZI Research Center for Information Technology, Karlsruhe, Germany floegel@fzi.de

² is with Facultad de Ingeniería, Universidad de Buenos Aires, Buenos Aires, Argentina

³ is with the Institute of Control Systems at Karlsruhe Institute of Technology, Karlsruhe, Germany soeren.hohmann@kit.edu

However, the distinction and consideration are essential for successful deployment in real-world environments [19]. Thus, we propose to disentangle the policy’s uncertainty measures and adapt the robot’s behavior in the crowd according to the confidence in the decision-making. As the main contribution of this work, (i) we augment the PPO algorithm to handle observation-dependent variance while keeping stable training and good exploration and exploitation trade-off. (ii) We incorporate and compare the suitability of MC-Dropout and Deep Ensembles for disentangling uncertainty estimation into epistemic, aleatoric, and predictive uncertainty. Consequently, (iii) we propose to change the robot behavior in uncertain interaction situations with humans to reduce collisions and negative impact. (iv) We demonstrate the effectiveness of our architecture in simulation.

II. BACKGROUND

A. Uncertainty Estimation in Machine Learning

Estimating the uncertainty can be distinguished into sample-free and sample-based methods, e.g., MC-Dropout or Ensembles, which require multiple forward passes [42]. Ensemble methods consist of a set of multiple models trained with different weight initializations. The variance of the different model predictions can be considered as Bayesian uncertainty estimates [42]. MC-Dropout randomly drops neurons during training and testing to form different models and combine their predictions as Bayesian uncertainty estimation [43]. The uncertainty estimates are further distinguished between the aleatoric, epistemic, and predictive uncertainty [44, 45]. Aleatoric uncertainty arises from the stochastic nature of the environment and can not be reduced. The three main sources in DRL are stochasticity in observation, actions, and rewards [19]. Epistemic uncertainty arises from limited knowledge gathered in training and accounts for the lack of knowledge of a policy but can be reduced with more training samples [19, 42]. *Predictive uncertainty* summarises the effects of aleatoric and epistemic uncertainty [44]. In decision making, aleatoric and epistemic uncertainty are disentangled for the DQN algorithm in [17, 18] but not adapted for actor-critic algorithms with continuous action space such as PPO [26] which is challenging [13].

B. Safety in Social Navigation

DRL-based social navigation approaches can be categorized based on the robot’s exhibited social behavior into social collision avoidance with a lack of social aspects, socially aware approaches with a predefined social behavior, and Socially Integrated (SI) where the robot’s behavior is adaptive to human behavior and emerges through interaction [8]. Early works proposed a Probability of Collision (POC) distribution in combination with a model-predictive controller (MPC) for safe and uncertainty-aware action selection [46, 47]. [47] uses MC-Dropout and bootstrapping to estimate the POC distribution for a risk-aware exploration in model-based DRL. An ensemble of LSTMs is used in [46] in combination with MC-Dropout and bootstrapping to estimate the distribution. A risk function is proposed in [5] to capture

the POC to prioritize humans with a higher risk of collision. However, a learned POC can be uncertain and does not reflect the policy uncertainty in the action selection. Other approaches use the uncertainty in human trajectory prediction for risk-aware planning [2, 9]. Such approaches are highly susceptible to the stochasticity of noise and the unobserved intentions of the external agents, which is addressed in [48] with a model-based DRL approach by estimating the aleatoric uncertainty of the trajectory prediction. A risk-map-based approach with human position prediction and probabilistic risk areas instead of hard collision avoidance is proposed in [15] to address dynamic human behavior and static clutter. Safety zones around humans are proposed in [24, 49, 50] to increase the minimum distance between the robot and humans. To overcome the problem of occluded humans, the social inference mechanism with a variational autoencoder to encode human interactions is incorporated in [16]. A risk-conditioned distributional SAC algorithm that learns multiple policies concurrently is proposed in [20]. The distributional DRL learns the distribution over the return and not only the expected mean, and the risk measure is a mapping from return distribution to a scalar value. Other works estimate uncertainty from environmental novelty [51], which does not translate to policy uncertainty. A resilient robot behavior for navigation in unseen uncertain environments with collision avoidance is addressed in [13]. An uncertainty-aware predictor for environmental uncertainty is proposed to learn an uncertainty-aware navigation network in prior unknown environments.

To our knowledge, no existing model-free DRL approaches consider the uncertainty in action selection and distinguish between epistemic and aleatoric uncertainty, which is crucial for safe and risk-aware decision-making.

III. PRELIMINARIES

Throughout this paper, a dynamic object in the environment is generally referred to as an agent, either a robot or a human, and a policy determines its behavior. Variables referred to the robot are indexed with x^0 , and humans with x^i with $i \in 1, \dots, N - 1$. A scalar value is denoted by x and a vector by \mathbf{x} .

A. Problem Formulation

The navigation task of one robot toward a goal in an environment of $N - 1$ humans is a sequential decision-making problem and can be modeled as Partially Observable Markov Decision Process (POMDP) [8, 10, 52, 53] and solved with a DRL framework [54]. The POMDP is described with a 8-tuple $(\mathcal{S}, \mathcal{A}, \mathcal{T}, \mathcal{O}, \Omega, \mathcal{T}_0, R, \gamma)$. We assume the state space \mathcal{S} and action space \mathcal{A} as continuous. The transition function $\mathcal{T} : \mathcal{S} \times \mathcal{A} \times \mathcal{S} \rightarrow [0, 1]$ describes the probability transitioning from state $s_t \in \mathcal{S}$ to state $s_{t+1} \in \mathcal{S}$ for the given action $\mathbf{a}_t \in \mathcal{A}$. With each transition, an observation $\mathbf{o}_t \in \mathcal{O}$ and a reward $R : \mathcal{S} \times \mathcal{A} \rightarrow \mathbb{R}$ is returned by the environment. The observation \mathbf{o}_t is returned with probability $\Omega(\mathbf{o}_t | s_{t+1}, \mathbf{a}_t, s_t)$ depending on the sensors. The initial state distribution is denoted by \mathcal{T}_0 while $\gamma \in [0, 1)$ describes the discount

factor. Every agent is completely described with a state $\mathbf{s}_t^i = [\mathbf{s}_t^{i,o}, \mathbf{s}_t^{i,h}]$ at any given time t . The state is separated into an observable part $\mathbf{s}_t^{i,o} = [\mathbf{p}, \mathbf{v}, r]$ with position \mathbf{p} , velocity \mathbf{v} , and radius r and unobservable, hidden part, $\mathbf{s}_t^{i,h} = [\mathbf{p}_g, v_{\text{pref}}, \psi_{\text{pref}}, r_{\text{prox}}]$ with goal position \mathbf{p}_g , preferred velocity v_{pref} , preferred orientation ψ_{pref} , and a proxemic radius r_{prox} according to Hall’s proxemic theory [55]. The world state $\mathbf{s}_t = [\mathbf{s}_t^0, \dots, \mathbf{s}_t^{N-1}]$ represents the environment at time t . One episode’s trajectory τ is the sequence of states, observations, actions, and rewards within the terminal time T . The return of one episode $\mathcal{R}(\tau) = \sum_{t=0}^T \gamma^t R_t$ is the accumulated and discounted reward R_t . The central objective is to learn the optimal robot policy π^* which maximizes the expected return:

$$\mathcal{T}(\tau|\pi) = \mathcal{T}(\mathbf{s}_0) \prod_{t=0}^T \mathcal{T}(\mathbf{s}_{t+1}|\mathbf{s}_t, \mathbf{a}_t)\pi(\mathbf{a}_t|\mathbf{o}_t) \quad (1)$$

$$\mathbb{E}_{\tau \sim \pi} [\mathcal{R}(\tau)] = \int_{\tau} \mathcal{T}(\tau|\pi) \mathcal{R}(\tau) \quad (2)$$

$$\pi^*(\mathbf{a}|\mathbf{o}) = \arg \max_{\pi} \mathbb{E}_{\tau \sim \pi} [\mathcal{R}(\tau)] \quad (3)$$

Considering a stochastic environment, $\mathcal{T}(\tau|\pi)$ is the probability of a trajectory starting in \mathbf{s}_0 with the probability \mathcal{T}_0 .

We follow our previous framework of a socially integrated navigation paradigm and use the reward system and observation as stated in [8] to learn a navigation policy from scratch that is adaptive to human behavior and leverages implicit social behavior instead of an explicit predefined behavior. The action of the policy is a velocity v_t and delta heading $\Delta\theta_t$ command.

IV. APPROACH

This section describes the incorporated uncertainty measurements and the uncertainty-aware action selection for collision avoidance. First, we introduce ODV into the PPO algorithm. Subsequently, we perform uncertainty estimations with MC-Dropout and Deep Ensembles within the DRL network. Finally, we provide a Probability of Collision (POC) estimation based on the uncertainty measurements for risk-aware action selection in novel and perturbed environments.

A. Observation-Dependent Variance

In standard implementations of PPO, e.g. *Stables Baselines3* [28], the actor outputs multivariate Gaussian distributed actions $\mathcal{N}(\boldsymbol{\mu}_a(\mathbf{o}_t), \boldsymbol{\sigma}_a^2)$ with an observation dependent mean but a parameterized variance, independent from observation. An observation-independent variance does not allow for aleatoric uncertainty estimation of the action selection process [13]. We, therefore, adapt the actor network and incorporate a linear layer that outputs the observation-dependent variances for the action as $\log(\boldsymbol{\sigma}_a)$. This leads to a multivariate Gaussian distributed policy $\mathcal{N}(\boldsymbol{\mu}_a(\mathbf{o}_t), \boldsymbol{\sigma}_a^2(\mathbf{o}_t))$ where both the mean and variance of the policy depend on the observation. However, using ODV leads to stability problems during training. First, the variance can be arbitrarily large, which can cause the normal distribution to lose its shape, become a uniform distribution, and disrupt learning

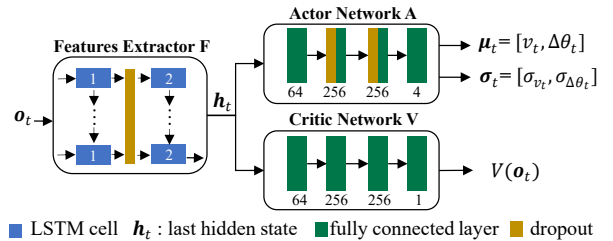


Fig. 2: Our ODV-PPO network, a common actor-critic architecture, with a shared features extractor and separated actor and value networks. The actor and the features extractor contain dropout layers. The actor outputs an observation-dependent mean and variance.

because actions are sampled randomly. Second, policy updates can lead to high variances at the late stages of training, which, by sampling, may lead to a sequence of poor actions, a series of bad updates, and, finally, performance collapse. We propose to use variance clamping for the first problem to prevent the deformation of the normal distribution by limiting the maximum variance. A grid search for the clamping values was done, and the highest maximum clamping value that did not cause collapse and still resembled a normal distribution was chosen. The second problem is addressed by modifying the PPO loss and incorporating the Mean Squared Error (MSE) loss of the variance

$$\mathcal{L}_{\theta}^{\sigma}(\pi) = \frac{t}{T} \cdot \lambda_{\sigma} \cdot \frac{1}{B} \sum_{i=1}^B \frac{1}{2} \cdot \left\| \begin{bmatrix} \sigma_{\Delta\theta_i}^2 \\ \sigma_{v_i}^2 \end{bmatrix} - \begin{bmatrix} 0 \\ 0 \end{bmatrix} \right\|^2 \quad (4)$$

where $\frac{t}{T}$ accounts for exploration-exploitation trade-off with the current timestep t and the total training timesteps T and batch size of B . The constant λ_{σ} scales the variance loss to be proportional to the policy loss and assigns importance to the variance loss and the MSE loss of the variance with respect to zero. This leads to total policy loss

$$\mathcal{L}_{\theta}(\pi) = \mathcal{L}_{\theta}^{\text{CLIP}}(\pi) + \mathcal{L}_{\theta}^{\sigma}(\pi) \quad (5)$$

where $\mathcal{L}_{\theta}^{\text{CLIP}}(\pi)$ is the PPO clipping loss. We refer to the full model as Observation-Dependent Variance PPO (ODV-PPO).

B. Uncertainty Estimation

1) *MC-Dropout*: We include dropout for approximating Bayesian inference in deep Gaussian processes during testing, named MC-Dropout [43], in two network sections. In the 2-layer LSTM features extractor and in the hidden layers of the actor-network, as depicted in Fig. 2. The critic network does not contain a dropout to avoid instabilities in the target value [45]. The policy is first trained with dropout probability p_{train} , and in testing, the samples are drawn with a higher dropout p_{test} to estimate the uncertainty. We sample K independent policy predictions with dropout of the action distribution $\boldsymbol{\mu}_k, \boldsymbol{\sigma}_k = \pi(\cdot|\mathbf{o}_t)$ for an observation at time step t . Subsequently, we calculate the uncertainties as proposed in [18] from the individual samples. The epistemic uncertainty is estimated with the variance of the means, with

$$\mathbf{u}^{\text{ep}} = \mathbb{V}[\boldsymbol{\mu}] \approx \frac{1}{K} \sum_{k=1}^K (\boldsymbol{\mu}_k - \bar{\boldsymbol{\mu}})^2 \quad (6)$$

where $\bar{\mu}_k$ is the average of the mean predictions obtained with dropout at time t . Additionally, we calculate the mean over the variances, which represents the aleatoric uncertainty

$$\mathbf{u}^{\text{al}} = \mathbb{E}[\boldsymbol{\sigma}^2] \approx \frac{1}{K} \sum_{k=1}^K \boldsymbol{\sigma}_k^2 \quad . \quad (7)$$

Note, both uncertainty measurements are vectors with the dimension of the action space.

2) *Deep Ensembles*: For Deep Ensembles, K networks are trained separately with different weight initialization and in environments with different seeds. A single network in the ensemble has the same architecture as in Fig. 2 and trained in the same way as for MC-Dropout. The dropout is used in the training for regularization but not used to calculate uncertainty measurements. In testing, each model of the ensemble gets the same observation. Thus, we generate K independent samples of the mean and variance of the actions. The epistemic uncertainty is then calculated with (6) and the aleatoric with (7).

3) *Features Extractor Uncertainty*: In addition to the epistemic and aleatoric uncertainty in the actor network, we estimate the predictive uncertainty of the features extractor, which does not distinguish between aleatoric and epistemic uncertainty. We distinguish between the predictive features uncertainty estimation with MC-Dropout and with the deep ensembles method.

For MC-Dropout, we get K samples of the hidden state \mathbf{h}_t at each time step t to estimate the uncertainty. Based on the K features vectors, we estimate a degree of uncertainty based on the method proposed in [56] and based on the element-wise variance in the features vector \mathbf{h}_t at each time step. This features variance vector is

$$\mathbb{V}(\mathbf{h}) = \begin{bmatrix} \mathbb{V}[h_1] \\ \vdots \\ \mathbb{V}[h_D] \end{bmatrix} = \begin{bmatrix} \frac{1}{K} \sum_{i=1}^K (h_{1,i} - \bar{h}_1)^2 \\ \vdots \\ \frac{1}{K} \sum_{i=1}^K (h_{D,i} - \bar{h}_D)^2 \end{bmatrix} \quad (8)$$

where D is the dimension of \mathbf{h} and $h_{d,i}$ is the d -th features vector element of the i -th sample from the K forward passes, and $\bar{h}_d = \frac{1}{K} \sum_{i=1}^K h_{d,i}$ is the mean for each element over the samples. During training, the minimum and maximum of each element in the features vector are tracked as h_d^{\min} and h_d^{\max} . Based on these values, an upper bound of the variance $\mathbb{V}[h_d]^{\max} = \frac{(h_d^{\max} - h_d^{\min})^2}{12}$ is calculated for each element, which occurs when the distribution follows a uniform distribution. Since the dimension of the features vector is commonly very high, a mapping function $g(\cdot) : \mathbb{R}^d \rightarrow \mathbb{R}$ is used to map the variance to a degree of uncertainty u^{feat} as proposed in [56]:

$$u^{\text{feat}} = g(\mathbb{V}(\mathbf{h})) = \sum_{d=1}^D \frac{\mathbb{V}(h_d)}{\sum_{d=1}^D \mathbb{V}(h_d)} \frac{\mathbb{V}(h_d)}{\mathbb{V}[h_d]^{\max}} \quad (9)$$

where $\mathbb{V}(h_d)$ is the d -th element of the features variance vector and $\mathbb{V}[h_d]^{\max}$ is used to normalize the uncertainty.

For deep ensembles, the uncertainty mapping is performed with the average of the features uncertainty

$$u^{\text{feat}} = g(\mathbb{V}(\mathbf{h})) = \frac{1}{D} \sum_{d=1}^D \mathbb{V}(h_d) \quad . \quad (10)$$

Using (9) would require training the ensemble models in parallel in the same environment, which is computationally heavy for a large K .

C. Uncertainty-Aware Action Selection

To avoid collision in scenarios where the robot is uncertain about action selection, we incorporate the uncertainty measurements into a POC estimation for safe action selection. For POC estimation, we investigated the application of a sigmoid function, training a Probability of Collision Network (PCN), and a threshold function, with the uncertainties as input. The PCN was trained in a similar manner as [46], but is too sensitive to the perturbation and activating itself easily in non-risky scenarios. Additionally, the sigmoid function could not be parameterized unambiguously. The best results were achieved by the threshold function

$$\mathbb{P}(\text{col}) = \begin{cases} 1, & \text{if } (c_{\text{ep}} \vee c_{\text{feat}}) \wedge c_{\text{prox}} \wedge c_{\text{ap}} \\ 0, & \text{otherwise} \end{cases} \quad (11)$$

which flags if the uncertainty condition, distance analysis and a scenario measure turn true. The uncertainty conditions indicate if the heading epistemic $c_{\text{ep}} = \mathbb{1}[u_{\text{head}}^{\text{ep}} > \lambda_{\text{ep}}]$ or the predictive feature uncertainty $c_{\text{feat}} = \mathbb{1}[u^{\text{feat}} > \lambda_{\text{f}}]$ are beyond a threshold. To analyze the trend of uncertainty in the trajectory, we smooth the noisy step-wise uncertainty estimates by windowing them over w previous steps. The proximity condition flags $c_{\text{prox}} = \mathbb{1}[(d_t^{0,j} + \beta_1 \cdot |\Delta v_t^{0,j}|) < \lambda_{\text{prox}}]$ scenarios with close distance $d_t^{0,j}$ to another human and takes into account the relative velocity $\Delta v_t^{0,j}$ to the nearest human. The approach condition $c_{\text{ap}} = \mathbb{1}[d_{t-1}^{0,j} \leq \hat{d}_t^{0,j}]$ considers that once the robot is moving away from the human, the risky scenario was averted.

With the POC, a risk-aware action selection can be proposed by either reducing the velocity or using a cautious policy when the POC is high. Since reducing the velocity is not always the best alternative, particularly when the other humans move fast [46], we propose to use a cautious policy. According to the social navigation taxonomy in [8], we propose to follow a social collision avoidance strategy in high-risk scenarios instead of a socially aware or socially integrated strategy and focus on physical collision avoidance in the first regard. We use the Optimal Reciprocal Collision Avoidance (ORCA) [57] as a collision avoidance strategy. To increase the caution, the radius of the surrounding humans

TABLE I: ODV-PPO Hyperparameters

Parameter	Value	Parameter	Value
variance factor λ_{σ}	0.1	dropout rate p_{train}	0.1
variance clamping min	-20	dropout rate p_{test}	0.5
variance clamping max	0.25	samples/models K	20

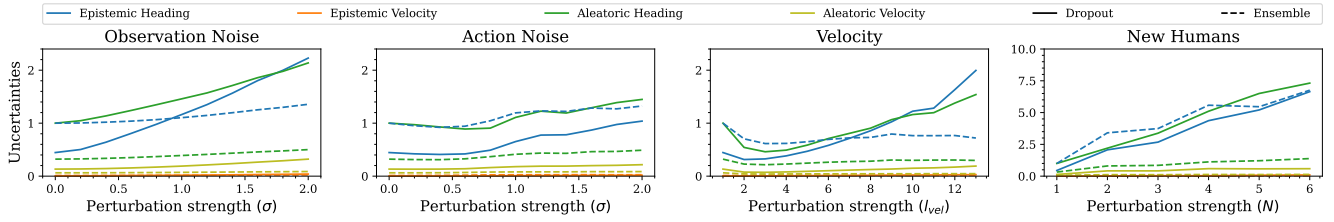


Fig. 3: Normalized and episodic mean values of epistemic and aleatoric uncertainty estimation using the MC-Dropout and deep ensemble approach.

is assumed to be 1.5 times bigger as observed, promoting trajectories away from the real human radius.

V. EVALUATION

In this section, we evaluate and compare the uncertainty measures in different scenarios and for different sources of perturbations. In addition, we benchmark our approach against the uncertainty unaware SI approach proposed in [8], which is only trained with PPO.

A. Experimental Setup

We use the gymnasium environment from our previous work in [8] to train and evaluate the navigation policies. The ODV-PPO based policy and the uncertainty measurements are implemented in *Stables Baselines3* [28] using the PPO hyperparameters from [8] and the newly introduced hyperparameters from Table I.

We consider two scenario configurations, a position swap scenario where the human position is randomly sampled on a circle with 7 m radius and a heterogeneous interactive circle crossing scenario as in [8] where each human has its individual proxemic radius. All policies are trained in a position swap scenario with one human. The agent radius is $r = 0.3$ m and the human proxemic radius is sampled with $r_{\text{prox}} = \mathcal{U}(0.3, 0.4)$. However, they are evaluated in both scenarios for 100 episodes per experiment. In addition, to analyze the uncertainty measurements, the position swap scenario is systematically expanded with perturbations, noise, and more humans. We stimulate aleatoric uncertainty with observation and action noise and epistemic uncertainty with an increased velocity of humans and an increased number of humans. Observation noise is modeled with additive Gaussian noise $\mathcal{N}(\mathbf{0}, I \cdot \sigma_{\text{obs}}^2)$. Action noise for the heading is modeled with additive Gaussian noise $\mathcal{N}(0, \sigma_{\text{head}}^2)$ and the velocity is scaled with a uniformly sampled factor $\mathcal{U}(1 - \sigma_{\text{vel}}, 1)$ with $\sigma_{\text{vel}} \leq 1$ to simulate terrain grip and avoid actions with negative velocity. The epistemic uncertainty is introduced through scaling the preferred velocity $l_{\text{vel}} \cdot v_{\text{pref}}^i$ of humans

and adding multiple humans into the environment to extend the position swap scenario into a circle-crossing scenario.

B. Results

1) *Training and Generalization*: Training the navigation policy with dropout and ODV-PPO leads to a faster convergence to a higher reward in comparison to PPO and PPO with dropout, throughout 10 seeds. To evaluate the capability to generalize and handle perturbed and OOD environments, we compare the ODV-PPO policy and our full approach with uncertainty aware safe action selection against the SI [8] approach in Table II. The position swap scenario is perturbed with an offset $\mathcal{U}(0, 0.5)$ to the start and goal position, the agent radius is $r_i = \mathcal{U}(0.3, 0.6)$, and the human proxemic radius is $r_{\text{prox}} = \mathcal{U}(0.3, 0.8)$. In the perturbed environment, the ODV-PPO approach always reaches the goal and has a higher average return. In the OOD scenario, circle crossing, both approaches cause many collisions and have low returns. Our proposed full model always reaches the goal and receives the highest average return.

TABLE II: Benchmarking in perturbed and OOD environments

Env. pos.	Approach	Goal(%)	Coll. (%)	Timeout (%)	Prox. Violations	Return
Swap	SI [8]	81	17	2	363	-1.1 ± 3.38
	ODV-PPO	100	0	0	219	2.06 ± 2.60
circle crossing	SI [8]	67	32	1	1060	0.14 ± 3.24
	ODV-PPO	68	32	0	966	0.837 ± 3.40
	Full	100	0	0	189	2.38 ± 2.6

2) *Disentangling Uncertainty Estimation*: We evaluate the MC-Dropout and Deep Ensemble approach with different perturbation sources and strengths and estimate the uncertainties in each step. Observation and action noise is $\sigma_{\text{head}}, \sigma_{\text{vel}}, \sigma_{\text{obs}} \in [0, 0.2, \dots, 2]$, velocity scaling factor is $l_{\text{vel}} \in [1, \dots, 8]$, and new humans are $N \in [2, \dots, 7]$. The estimated aleatoric and epistemic uncertainties are depicted in Fig. 3. For both approaches, the results show that the velocity uncertainty is low and flat compared to the heading uncertainty, which increases approximately linearly, and new humans cause the highest uncertainty. In addition, the MC-Dropout approach is capable of disentangling the source of the uncertainty, but we also observed that a proper dropout rate p_{test} is crucial for this capability. In contrast, the deep ensemble approach always has high epistemic uncertainty and cannot distinguish between aleatoric and epistemic uncertainty. The results are also aggregated in Table III for the normalized rate of change of the uncertainties for the perturbation. The normalized value is $\frac{\Delta U}{\Delta \sigma} = \frac{1}{u_{\sigma(0)}} \frac{u_{\sigma(\text{max})} - u_{\sigma(0)}}{\sigma(\text{max}) - \sigma(0)}$ with the maximum perturbation strength $\sigma(\text{max})$, the mean uncertainty $u_{\sigma(\text{max})}$ per strength, and the mean uncertainty $u_{\sigma(0)}$ in the unperturbed environment of the episodes.

To analyze the trend of uncertainty as the robot approaches and interacts with the human, the mean uncertainty \bar{u}_w

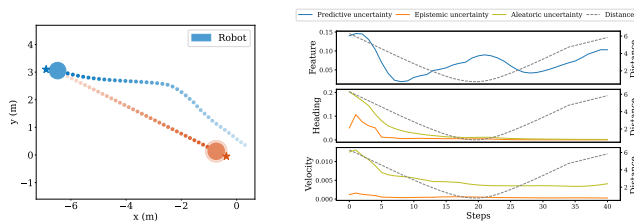


Fig. 4: Windowed uncertainty estimates ($w = 4$) using MC-Dropout approach. Position swap scenario with start and goal position perturbation.

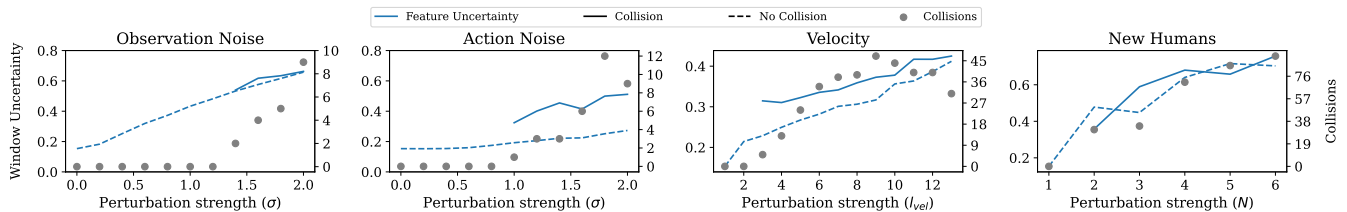


Fig. 5: Windowed predictive uncertainty of features extractor using MC-Dropout approach on step before collision or at closest distance.

over a window of the last $w = 4$ steps is evaluated. The experiments show that the predictive uncertainty increases for both approaches in close situations, as exemplified in Fig. 4, but the action uncertainty is low. For MC-Dropout approach, the windowed predictive feature uncertainty is one step before collision (if occurred) higher for action and velocity noise compared to the step of minimum distance (if no collision occurred) as depicted in Fig. 5. However, there is no distinction for the deep ensemble approach, which is additionally less sensitive. In addition, the results show that the number of collisions increases with the perturbation strength, as depicted with grey dots in Fig. 5.

TABLE III: Normalized aggregated uncertainty estimates

Uncertainties	Observation Noise		Action Noise		Velocity		New Humans	
	Dropout	Ensemble	Dropout	Ensemble	Dropout	Ensemble	Dropout	Ensemble
Predictive Feature	1.84	0.11	0.87	0.03	0.20	0	0.65	0.38
Aleatoric Heading	0.57	0.28	0.22	0.26	0.04	0	0.90	0.47
Epistemic Heading	2.00	0.18	0.67	0.16	0.25	0	1.99	0.82
Aleatoric Velocity	0.71	0.19	0.31	0.18	0.03	0	0.49	0.17
Epistemic Velocity	4.08	0.49	1.46	0.64	0.39	0.02	3.01	0.30

3) *Uncertainty-Aware Action Selection*: For collision avoidance, the uncertainty is converted into a POC estimation using (11) with the threshold constants for MC-Dropout $\lambda_{ep} = 0.03$, $\lambda_f = 0.3$, $\lambda_{prox} = 0.9$, $\beta_1 = 0.5$ and deep ensemble $\lambda_{ep} = 0.08$, $\lambda_f = 0.0033$, $\lambda_{prox} = 0.9$, $\beta_1 = 0.5$ by analyzing uncertainty-perturbation correlations, e.g. Fig. 3 and Fig. 5. This ensures that the safe action selection only activates in steps or scenarios with a high risk of collision. The results show that the MC-Dropout is more suitable for safe action selection across all perturbations and strengths as aggregated in Fig. 6 with the relative percentage of prevented collisions compared to no safe action selection.

C. Discussion

Using dropout and ODV in PPO leads to better policy quality in terms of generalization and training convergence. If the basic structure of the scenario is the same as in training, the policy generalizes better with ODV exploration and dropout. However, if the scenario is entirely different, as it can occur in reality, the generalization is not sufficient and the policy predicts overconfident actions. A predictive uncertainty does not correlate with high uncertainty in decision-making as visualized in Fig. 4 but can reveal risky scenarios. This further confirms the need for uncertainty measurements in decision-making and not only to detect novel scenarios. The comparison of the uncertainty methods shows that the MC-Dropout approach can better distinguish between aleatoric and epistemic uncertainty with properly

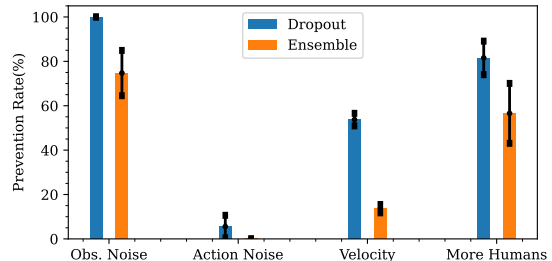


Fig. 6: Relative percentage of prevented collisions with safe action selection.

selected dropout rate in inference and has additionally higher sensitivity to noise. The aleatoric uncertainty is sensitive to noises, showing that it associates the uncertainty type with the source of uncertainty. However, since all perturbed scenarios are partially OOD scenarios and the policy was only trained in a very simple scenario, the epistemic uncertainty is generally high. The results show that the perturbations sources have varying impacts on decision-making, whereas they impact equally in predictive uncertainty. The policy is more uncertain about the heading throughout all perturbations, which is crucial for safe action selection and future design of DRL policies. More humans in the environment cause the highest uncertainty in decision-making, but collisions are most difficult to prevent in the case of action noise. However, both approaches have the drawback of sample-based uncertainty estimation, which either requires multiple forward passes for dropout or storing multiple models in parallel for the ensemble approach.

VI. CONCLUSIONS

This paper incorporated and disentangled epistemic, aleatoric, and predictive uncertainty measurements in a DRL network with a safe action selection for perturbation robustness in social navigation. We integrated observation-dependent variance and dropout into the PPO algorithm with adaptations in the action network and loss function. This leads to a better generalization with faster convergence and enables disentangling the aleatoric and epistemic uncertainty in decision-making. The results show that the MC-Dropout-based approach is superior for uncertainty estimation and, in combination with the proposed safe action selection, can avoid more collisions than the ensemble approach. In addition, the predictive uncertainty in perturbed environments can be high, although the robot is sure about selecting the action. Consequently, the uncertainty in the decision-making must be considered to detect when and why the robot is uncertain. Future works develop sample-free methods.

REFERENCES

- [1] F. Cavallo, F. Semeraro, L. Fiorini, G. Magyar, P. Sinčák, and P. Dario, "Emotion modelling for social robotics applications: A review," *Journal of Bionic Engineering*, vol. 15, no. 2, pp. 185–203, 2018.
- [2] E. Alao and P. Martinet, "Uncertainty-aware navigation in crowded environment," in *17th International Conference on Control, Automation, Robotics and Vision (ICARCV)*. IEEE, 2022, pp. 293–298.
- [3] B. Varga, D. Yang, M. Martin, and S. Hohmann, "Cooperative decision-making in shared spaces: Making urban traffic safer through human-machine cooperation," in *IEEE 21st Jubilee International Symposium on Intelligent Systems and Informatics (SISY)*, 2023.
- [4] T. Genevois, A. Spalanzani, and C. Laugier, "Interaction-aware predictive collision detector for human-aware collision avoidance," in *2023 IEEE Intelligent Vehicles Symposium (IV)*. IEEE, 2023, pp. 1–7.
- [5] X. Sun, Q. Zhang, Y. Wei, and M. Liu, "Risk-aware deep reinforcement learning for robot crowd navigation," *Electronics*, vol. 12, no. 23, p. 4744, 2023.
- [6] S. Guillén-Ruiz, J. P. Bandera, A. Hidalgo-Paniagua, and A. Bandera, "Evolution of socially-aware robot navigation," *Electronics*, 2023.
- [7] C. Mavrogiannis, F. Baldini, A. Wang, D. Zhao, P. Trautman, A. Steinfeld, and J. Oh, "Core challenges of social robot navigation: A survey," *ACM Transactions on Human-Robot Interaction*, vol. 12, no. 3, pp. 1–39, 2023.
- [8] D. Flögel, L. Fischer, T. Rudolf, T. Schürmann, and S. Hohmann, "Socially integrated navigation: A social acting robot with deep reinforcement learning," 2024. [Online]. Available: <https://arxiv.org/abs/2403.09793>
- [9] M. Golchoubian, M. Ghafurian, K. Dautenhahn, and N. L. Azad, "Uncertainty-aware drl for autonomous vehicle crowd navigation in shared space." [Online]. Available: <http://arxiv.org/pdf/2405.13969v1>
- [10] K. Zhu and T. Zhang, "Deep reinforcement learning based mobile robot navigation: A review," *Tsinghua Science and Technology*, vol. 26, no. 5, pp. 674–691, 2021.
- [11] K. Ryu and N. Mehr, "Integrating predictive motion uncertainties with distributionally robust risk-aware control for safe robot navigation in crowds." [Online]. Available: <http://arxiv.org/pdf/2403.05081v1>
- [12] A. Sedlmeier, T. Gabor, T. Phan, and L. Belzner, "Uncertainty-based out-of-distribution detection in deep reinforcement learning," *Digitale Welt*, vol. 4, no. 1, pp. 74–78, 2020. [Online]. Available: <https://link.springer.com/article/10.1007/s42354-019-0238-z>
- [13] T. Fan, P. Long, W. Liu, J. Pan, R. Yang, and D. Manocha, *Learning Resilient Behaviors for Navigation Under Uncertainty*. Piscataway, NJ: IEEE, 2020. [Online]. Available: <https://ieeexplore.ieee.org/servlet/opac?punumber=9187508>
- [14] M. Everett, B. Lutjens, and J. P. How, "Certifiable robustness to adversarial state uncertainty in deep reinforcement learning," *IEEE Transactions on Neural Networks and Learning Systems*, vol. 33, no. 9, pp. 4184–4198, 2022. [Online]. Available: <http://arxiv.org/pdf/2004.06496v6>
- [15] H. Yang, C. Yao, C. Liu, and Q. Chen, "Rmrl: Robot navigation in crowd environments with risk map-based deep reinforcement learning," *IEEE Robotics and Automation Letters*, vol. 8, no. 12, 2023.
- [16] Y.-J. Mun, M. Itkina, S. Liu, and K. Driggs-Campbell, "Occlusion-aware crowd navigation using people as sensors," in *2023 IEEE International Conference on Robotics and Automation (ICRA)*. IEEE, 2023, pp. 12031–12037.
- [17] W. R. Clements, B. van Delft, B.-M. Robaglia, R. B. Slaoui, and S. Toth, "Estimating risk and uncertainty in deep reinforcement learning." [Online]. Available: <http://arxiv.org/pdf/1905.09638v5>
- [18] B. Charpentier, R. Senanayake, M. Kochenderfer, and S. Gunnemann, "Disentangling epistemic and aleatoric uncertainty in reinforcement learning," 2022. [Online]. Available: <https://arxiv.org/abs/2206.01558>
- [19] O. Lockwood and M. Si, "A review of uncertainty for deep reinforcement learning." [Online]. Available: <http://arxiv.org/pdf/2208.09052>
- [20] J. Choi, C. Dance, J.-e. Kim, S. Hwang, and K.-s. Park, "Risk-conditioned distributional soft actor-critic for risk-sensitive navigation," in *2021 IEEE International Conference on Robotics and Automation (ICRA)*. IEEE, 2021, pp. 8337–8344.
- [21] K. Zhu, B. Li, W. Zhe, and T. Zhang, "Collision avoidance among dense heterogeneous agents using deep reinforcement learning," *IEEE Robotics and Automation Letters*, vol. 8, no. 1, pp. 57–64, 2023.
- [22] V. Narayanan, B. M. Manoghar, R. P. RV, and A. Bera, "Ewaretnet: Emotion-aware pedestrian intent prediction and adaptive spatial profile fusion for social robot navigation," in *2023 IEEE International Conference on Robotics and Automation (ICRA)*. IEEE, 2023.
- [23] T. Zhang, T. Qiu, Z. Pu, Z. Liu, and J. Yi, "Robot navigation among external autonomous agents through deep reinforcement learning using graph attention network," *IFAC-PapersOnLine*, vol. 53, no. 2, pp. 9465–9470, 2020.
- [24] B. Xue, M. Gao, C. Wang, Y. Cheng, and F. Zhou, "Crowd-aware socially compliant robot navigation via deep reinforcement learning," *International Journal of Social Robotics*, 2023.
- [25] M. Everett, Y. F. Chen, and J. P. How, "Collision avoidance in pedestrian-rich environments with deep reinforcement learning," *IEEE Access*, vol. 9, pp. 10357–10377, 2021.
- [26] J. Schulman, F. Wolski, P. Dhariwal, A. Radford, and O. Klimov, "Proximal policy optimization algorithms," 20.07.2017.
- [27] T. Haarnoja, A. Zhou, K. Hartikainen, G. Tucker, S. Ha, J. Tan, V. Kumar, H. Zhu, A. Gupta, P. Abbeel, and S. Levine, "Soft actor-critic algorithms and applications." [Online]. Available: <http://arxiv.org/pdf/1812.05905v2>
- [28] Antonin Raffin, Ashley Hill, Adam Gleave, Anssi Kanervisto, Maximilian Ernestus, and Noah Dormann, "Stable-baselines3: Reliable reinforcement learning implementations," *Journal of Machine Learning Research*, vol. 22, no. 268, pp. 1–8, 2021.
- [29] Y. Tao, M. Li, X. Cao, and P. Lu, "Mobile robot collision avoidance based on deep reinforcement learning with motion constraints," *IEEE Transactions on Intelligent Vehicles*, pp. 1–11, 2024.
- [30] P. Long, T. Fan, X. Liao, W. Liu, H. Zhang, and J. Pan, "Towards optimally decentralized multi-robot collision avoidance via deep reinforcement learning." [Online]. Available: <http://arxiv.org/pdf/1709.10082v3>
- [31] X. Gao, S. Sun, X. Zhao, and M. Tan, "Learning to navigate in human environments via deep reinforcement learning," in *Neural Information Processing*, ser. Lecture Notes in Computer Science, T. Gedeon, K. W. Wong, and M. Lee, Eds. Cham: Springer International Publishing, 2019, vol. 11953, pp. 418–429.
- [32] D. Dugas, O. Andersson, R. Siegwart, and J. J. Chung, "Navdreams: Towards camera-only rl navigation among humans." [Online]. Available: <http://arxiv.org/pdf/2203.12299v1>
- [33] Q. Qiu, S. Yao, J. Wang, J. Ma, G. Chen, and J. Ji, "Learning to socially navigate in pedestrian-rich environments with interaction capacity," in *2022 International Conference on Robotics and Automation (ICRA)*. IEEE, 2022, pp. 279–285.
- [34] S. Yao, G. Chen, Q. Qiu, J. Ma, X. Chen, and J. Ji, "Crowd-aware robot navigation for pedestrians with multiple collision avoidance strategies via map-based deep reinforcement learning," in *2021 IEEE/RSJ International Conference on Intelligent Robots and Systems (IROS)*. IEEE, 2021, pp. 8144–8150.
- [35] B. Brito, M. Everett, J. P. How, and J. Alonso-Mora, "Where to go next: Learning a subgoal recommendation policy for navigation among pedestrians," 25.02.2021.
- [36] T. Fan, X. Cheng, J. Pan, D. Manocha, and R. Yang, "Crowdmove: Autonomous mapless navigation in crowded scenarios," 2018.
- [37] Z. Hu, J. Pan, T. Fan, R. Yang, and D. Manocha, "Safe navigation with human instructions in complex scenes," *IEEE Robotics and Automation Letters*, vol. 4, no. 2, pp. 753–760, 2019.
- [38] B. Chen, H. Zhu, S. Yao, S. Lu, P. Zhong, Y. Sheng, and J. Wang, "Socially aware object goal navigation with heterogeneous scene representation learning," *IEEE Robotics and Automation Letters*, vol. 9, no. 8, pp. 6792–6799, 2024.
- [39] J. Li, C. Hua, H. Ma, J. Park, V. Dax, and M. J. Kochenderfer, "Multi-agent dynamic relational reasoning for social robot navigation." [Online]. Available: <http://arxiv.org/pdf/2401.12275v1>
- [40] R. Guldenring, M. Gerner, N. Hendrich, N. J. Jacobsen, and J. Zhang, "Learning local planners for human-aware navigation in indoor environments," in *2020 IEEE/RSJ International Conference on Intelligent Robots and Systems (IROS)*. IEEE, 2020, pp. 6053–6060.
- [41] Z. Xie and P. Dames, "Drl-vo: Learning to navigate through crowded dynamic scenes using velocity obstacles," *IEEE Transactions on Robotics*, vol. 39, no. 4, pp. 2700–2719, 2023. [Online]. Available: <http://arxiv.org/pdf/2301.06512v2>

- [42] B. P. Charpentier, "Uncertainty estimation for independent and non-independent data," Ph.D. dissertation, Technische Universität München, 2024.
- [43] Y. Gal and Z. Ghahramani, "Dropout as a bayesian approximation: Representing model uncertainty in deep learning." [Online]. Available: <http://arxiv.org/pdf/1506.02142v6>
- [44] Y. Gal, "Uncertainty in deep learning." 2016. [Online]. Available: <https://api.semanticscholar.org/CorpusID:86522127>
- [45] O. Lockwood and M. Si, "A review of uncertainty for deep reinforcement learning," in *Proceedings of the AAAI Conference on Artificial Intelligence and Interactive Digital Entertainment*, vol. 18, no. 1, 2022, pp. 155–162.
- [46] Björn Lütjens, M. Everett, and J. P. How, "Safe reinforcement learning with model uncertainty estimates," in *2019 International Conference on Robotics and Automation (ICRA)*, 2019, pp. 8662–8668.
- [47] G. Kahn, A. Villaflor, V. Pong, P. Abbeel, and S. Levine, "Uncertainty-aware reinforcement learning for collision avoidance." [Online]. Available: <http://arxiv.org/pdf/1702.01182v1>
- [48] C. Diehl, T. Sievernich, M. Krüger, F. Hoffmann, and T. Bertram, "Umbrella: Uncertainty-aware model-based offline reinforcement learning leveraging planning," *arXiv preprint arXiv:2111.11097*, 2021.
- [49] L. Kästner, J. Li, Z. Shen, and J. Lambrecht, "Enhancing navigational safety in crowded environments using semantic-deep-reinforcement-learning-based navigation." [Online]. Available: <http://arxiv.org/pdf/2109.11288v1>
- [50] S. S. Samsani and M. S. Muhammad, "Socially compliant robot navigation in crowded environment by human behavior resemblance using deep reinforcement learning," *IEEE Robotics and Automation Letters*, vol. 6, no. 3, pp. 5223–5230, 2021.
- [51] C. Richter and N. Roy, "Safe visual navigation via deep learning and novelty detection," 2017.
- [52] Y. F. Chen, M. Liu, M. Everett, and J. P. How, "Decentralized non-communicating multiagent collision avoidance with deep reinforcement learning," in *2017 IEEE International Conference on Robotics and Automation (ICRA)*. IEEE, 2017, pp. 285–292.
- [53] C. Chen, Yuejiang Liu, Sven Kreiss, and Alexandre Alahi, *Crowd-Robot Interaction: Crowd-aware Robot Navigation with Attention-based Deep Reinforcement Learning*. Piscataway, NJ: IEEE, 2019.
- [54] A. B. Richard Sutton, "Reinforcement learning: An introduction: second edition," 2020.
- [55] E. T. Hall, *The hidden dimension*. New York: Anchor Books, 1996.
- [56] C. Kim, J.-K. Cho, H.-S. Yoon, S.-W. Seo, and S.-W. Kim, "Unicon: Uncertainty-conditioned policy for robust behavior in unfamiliar scenarios," *IEEE Robotics and Automation Letters*, vol. 7, no. 4, pp. 9099–9106, 2022.
- [57] J. van den Berg, S. J. Guy, M. Lin, and D. Manocha, "Reciprocal n-body collision avoidance," in *Robotics Research*, ser. Springer Tracts in Advanced Robotics, B. Siciliano, O. Khatib, F. Groen, C. Pradalier, R. Siegwart, and G. Hirzinger, Eds. Springer Berlin Heidelberg, 2011.